Optical and Quantum Electronics (2023) 55:258
https://doi.org/10.1007/s11082-022-04441-w

A theoretical approach towards designing of banana shaped non-fullerene chromophores using efficient acceptors moieties: exploration of their NLO response properties

Muhammad Khalid[1,2] · Samran Naseer[1,2] · Muhammad Suleman Tahir[3] · Iqra shafiq[1,2] · Khurram Shahzad Munawar[4] · Sara Figueirêdo de Alcântara Morais[5] · Ataualpa A. C. Braga[5]

Received: 11 July 2022 / Accepted: 27 November 2022 / Published online: 9 January 2023

Abstract

Current research has focused on utilization of non-fullerene based organic materials for the advancement of nonlinear optical (NLO) based technology. The reference compound (**DTPSR1**) was used in tailoring process to design seven new derivatives (**DTPSD2-DTPSD8**) via various acceptor moieties. The M06-2X level with 6-311G(d,p) basis set was used for assessing frontier molecular orbitals (FMOs), natural bonding orbital (NBO), nonlinear optical properties [average polarizability $<\alpha>$, first hyperpolarizability (β_{total}), second hyperpolarizability (γ_{total})], transition density matrix (TDM) and UV–Vis analyses of **DTPSR1** and **DTPSD2-DTPSD8**. The UV–Vis analysis indicated that the designed derivatives show comparable results (515.462–586.269 nm) with reference molecule (583.592 nm), except **DTPSD7**, that exhibited slight red shift (586.269 nm). Smaller LUMO–HOMO energy gaps were reported as in **DTPSD3** (3.53 eV), **DTPSD7** (3.53 eV) and **DTPSD8** (3.55 eV) as compared to **DTPSR1** (3.60 eV) which was further supported by TDM analysis. The global reactivity descriptors have also shown close correlation with LUMO–HOMO energy gaps; smaller value of energy gap showed lower hardness value 1.77 eV for **DTPSD3**, **DTPSD7** and **DTPSD8** and greater softness values 0.283 eV for **DTPSD3**, **DTPSD7** and 0.281 eV for **DTPSD8**, respectively. The hyper conjugative interactions, stability, and electron-transfer mechanism were elucidated by using NBO analysis. **DTPSD2-DTPSD8** also exhibited comparatively closer NLO results with **DTPSR1**. Among **DTPSD2–DTPSD8**, the highest $\langle\alpha\rangle$1439.16 a.u, β_{total} 189,720.546 a.u and γ_{total} 1.980890×10^{7} a.u were observed for **DTPSD7**. It is anticipated that our study would provide a springboard to attain the NLO materials exhibiting significant future applications such as in telecommunication, data storage and optical poling.

Keywords Hyperpolarizability · Carbazole based derivatives · Non-fullerene acceptors · DFT · D–π–A chromophores

✉ Muhammad Khalid
muhammad.khalid@kfueit.edu.pk; khalid@iq.usp.br

Extended author information available on the last page of the article

1 Introduction

Nonlinear optical (NLO) materials have recently attracted theoretical and experimental researchers due to their fascinating potential properties (Ahmad et al. 2018; Akram et al. 2018; Papadopoulos, Sadlej and Leszczynski 2006; Shahid et al. 2018). The NLO chromophores possess substantial applications in a wide range of disciplines i.e. nuclear research, medicine, chemical dynamics, solid-state physics, material sciences and biophysics (Eaton 1991). The NLO compounds are also becoming essential in various technologies particularly optical computing, optical communication, and dynamic image processing (Breitung et al. 2000; Peng and Yu 1994; Tsutsumi, Morishima and Sakai 1998). Therefore, multiple attempts are being made to explore various NLO materials comprising nanomaterials, organic and inorganic semiconductors, polymer frameworks and molecular dyes (Fonseca et al. 2018; Guo et al. 2018; Halasyamani and Zhang 2017; Yamashita 2011; Zhang et al. 2017). Some essential features to be NLO material are inexpensive production cost, small dielectric constant, significant photoelectric coefficient, and designing freedom. Organic compounds carrying hyperpolarizability have gained a lot of interest to be used in this field because of their environment friendly nature, ease of refining and formation (Nagarajan et al. 2017). Strong intramolecular charge transfer (ICT) is also an important property which arises due to electron density transfer from donor (D) to acceptor (A) via π-bridge to produce a substantial dipole moment among the molecule's ground and excited levels (Chemla 2012; Prasad and Williams 1991).

Significant NLO response in donor–acceptor (D-A) molecules can be described by using two-state model (Roy and Nandi 2015). As a general assumption, the basic framework of NLO molecule is mainly composed of donor (D) acceptor (A) pairs bonded via π-conjugated electron bridges (D–π–A). This type of configuration along with conjugated length is taken into consideration when selecting D–π–A chromophores (Janjua, Amin et al. 2012a; Janjua et al. 2012b; Khan et al. 2018, 2019a, b, c) as D and A entities are essential in generating considerable NLO response. In the majority of NLO compounds, electronic charge is delocalized in the π-bond framework and the first hyperpolarizability is associated to ICT (Chemla 2012; Prasad and Williams 1991). Numerous frameworks have been previously described in the literature particularly, D–π–A, D–A–π–A, A–π–D–π–A, D–π–π–A, D–π–A–π–D, D–A and D–D–π–A (Katono et al. 2014; Namuangruk et al. 2012; Panneerselvam et al. 2017; Wielopolski et al. 2013). For designing, an effective push–pull framework A–D–π–π–A and D–A–D–π–π–A based organic molecules have been developed by using appropriate D, π-linker and A moieties. The push–pull design minimize the charge recombination, bring alteration in charge dissociation, expansion in absorption to a higher wavelength, intensification in asymmetrical electronic distribution, and reduction in energy gap (E_{gap}) which results in magnificent NLO response (Haroon et al. 2017; Janjua 2010; Januja et al. 2012a, 2014, 2015a, b), Efficient designing of D–π–A molecules for their improved NLO applications is essential in current research work. Fullerenes have 3 dimensional cages like structure known to have outstanding NLO behavior because of their greater π-conjugated network and the substantial delocalization of charge (He and Li 2011). Fullerenes exhibit a number of profitable characteristics and their primary success in the area of organic photo electronics was reported. In spite of their success, many difficulties and disadvantages still exists in fullerenes that cannot be minimized without altering this preliminary class of acceptors. Over the last few years, the evolution of exchanging fullerene-based acceptors with non-fullerene acceptors (NFAs) has reinforced the field of optoelectronics to some level (Wadsworth et al. 2019). The NFAs have fundamental advantages comprising tunability of band gaps, light absorption, energy state validity and

planarity. Nowadays, these NFAs have expressed exceptional stability as compared to fullerene based acceptor molecules (Cheng et al. 2018). On the basis of these magnificent properties, our goal is to provide a theoretical viewpoint on NLO characteristics of NFAs organic materials. The NLO investigation of entitled NFA based reference molecule **DTPSR1** and its derivatives **DTPSD2-DTPSD8** might not be reported yet. Hence, to overcome this research gap, recent studies are done to design seven novel derivatives (**DTPSD2-DTPSD8**) of a reference compound (**DTPSR1**) to elaborate their NLO behavior by DFT and TD-DFT computations. We are optimistic that this research would be a new contribution for the researchers to further explore the NLO behavior of NFAs.

1.1 Computational procedure

DFT calculations are used to estimate electronic analysis, absorption spectra, and NLO parameters of **DTPSR1** and **DTPSD2-DTPSD8** chromophores. The quantum chemical investigations of these chromophores were carried out by using Gaussian 09 (Frisch and Clemente 2009) program package at M06-2X/6-311G(d,p) level of theory. By employing the above level and the same basis set (Khalid et al. 2021a, b), the NBO 3.1 software (Glendening and Weinhold 1998) was utilized for the natural bond orbital (NBO) analysis. The FMOs, TDM, and UV–Vis spectral analysis was computed via using (TD-DFT) at the same functional. The input files are generated by using GaussView 5.0, (Dennington, Keith and Millam 2016) while, Avogadro (Hanwell et al. 2012) and Chemcraft (Zhurko and Zhurko 2009) are used to evaluate the remaining data. The dipole moment is determined by using Eq. 1 (Valverde et al. 2018) and average polarizability $\langle a \rangle$ is calculated from the Eq. (2) (Barone and Cossi 1998).

$$\mu = \left(\mu_x^2 + \mu_y^2 + \mu_z^2\right)^{1/2} \tag{1}$$

$$< a > = 1/3\left(a_{xx} + a_{yy} + a_{zz}\right) \tag{2}$$

The following 9 hyperpolarizability tensors: β_{xxx}, β_{xyy}, β_{xzz}, β_{yyy}, β_{xxy}, β_{yzz}, β_{zzz}, β_{xxz} and β_{yyz} were found in the Gaussian output file and Eq. (3) (Tamer et al. 2016) is used to compute the magnitude of the first hyperpolarizability (β_{tot}).

$$\beta_{total} = \left(\beta_x^2 + \beta_y^2 + \beta_z^2\right)^{1/2} \tag{3}$$

The second hyperpolarizability is determined by utilizing the Eq. 4.

$$\gamma_{total} = \sqrt{\gamma_x^2 + \gamma_y^2 + \gamma_z^2} \tag{4}$$

where $\gamma_i = \frac{1}{15}\sum_j \left(\gamma_{ijji} + \gamma_{ijij} + \gamma_{iijj}\right) \quad i,j = \{x,y,z\}$.

2 Results and discussion

Self-assembly and molecular structure understanding is very critical for revealing optoelectronic properties of molecules. A highly efficient NFA namely CH1007 is a selenium analog of Y6 reported by Lin et al. (Lin et al. 2020) CH1007 holds proven track record of superior charge-transporting characteristics and phenomenal PCE of 17.08%. This study advocates

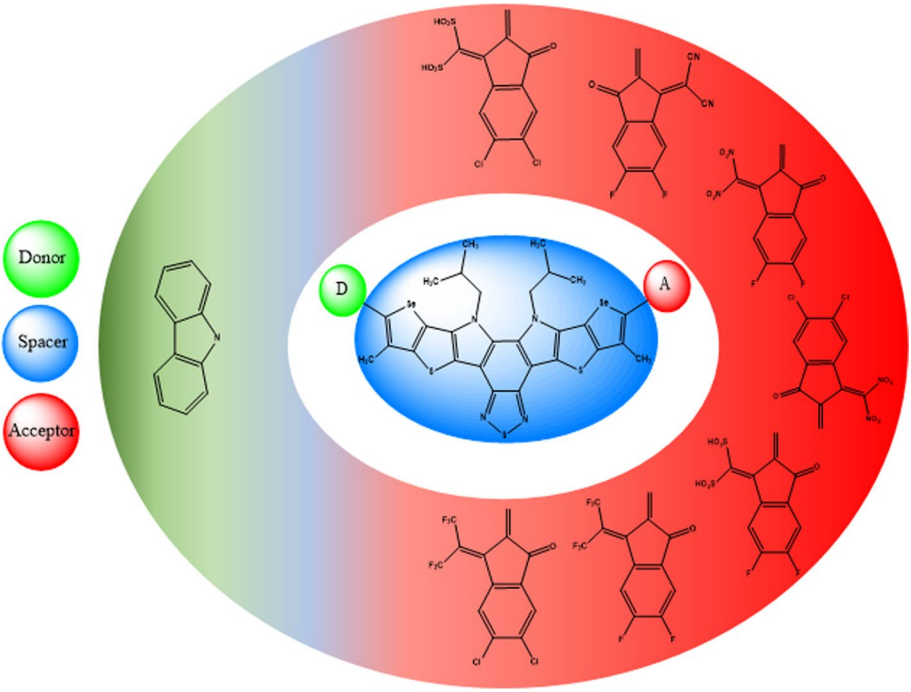

Scheme 1 Sketch map of designed compounds (**DTPSR1** and **DTPSD2- DTPSD8**)

the molecular structural tailoring of highly efficient CH1007 (named as **DTPSR1** in this study) NFA for their NLO response exploration and their utilization in NLO based applications. The reference molecule **DTPSR1** possessed an A-D-A architecture which is modified to D–π–A by replacing one end-capped unit with efficient electron donor carbazole moiety. Similarly, the second end-capped unit is modified with well-known reported end capped acceptor units and seven new compounds **DTPSD2** (2-(5,6-difluoro-2-methylene-3-oxo-2,3-dihydro-1*H*-inden-1-ylidene)malononitrile), **DTPSD3** (3-(dinitromethylene)-5,6-difluoro-2-methylene-2,3-dihydro-1*H*-inden-1-one), **DTPSD4** (5,6-difluoro-2-methylene-3-oxo-2,3-dihydro-1*H*-inden-1-ylidene)methanedisulfonic acid), **DTPSD5** (5,6-difluoro-2-methylene-3-(perfluoropropan-2-ylidene)-2,3-dihydro-1*H*-inden-1-one), **DTPSD6** (5,6-dichloro-2-methylene-3-(perfluoropropan-2-ylidene)-2,3-dihydro-1*H*-inden-1-one), **DTPSD7** (5,6-dichloro-2-methylene-3-oxo-2,3-dihydro-1*H*-inden-1-ylidene)methanedisulfonic acid), and **DTPSD8** (3.55 eV) having (5,6-dichloro-3-(dinitromethylene)-2-methylene-2,3-dihydro-1H-inden-1-one) are developed theoretically. These proposed compounds are divided into three fragments such as terminal donor, central core π-spacer and peripheral acceptor represented in Scheme 1 as D–π–A network.

The optimized molecule geometries of investigated compounds are shown in Fig. 1.

2.1 Frontier molecular orbitals (FMO) analysis

The FMOs is a good theory for predicting the chemical stability of the investigated compounds (Gunasekaran et al. 2008). The highest occupied molecular orbital (HOMO) and

the lowest unoccupied molecular orbital (LUMO) are significant quantum orbitals that influence UV–Vis spectra and chemical mechanisms. LUMO usually relates to the capability to accept electrons, while HOMO relates to the capability to donate electrons (Amiri et al. 2016). The chemical reactivity, dynamic stability, chemical softness, and rigidity of molecules are also anticipated by LUMO–HOMO energy gap (Khalid et al. 2017). Chemically hard molecules possess greater E_{LUMO}-E_{HOMO} energy gap are considered to have superior kinetic stability and reduced chemical reactivity. On the other hand, molecules

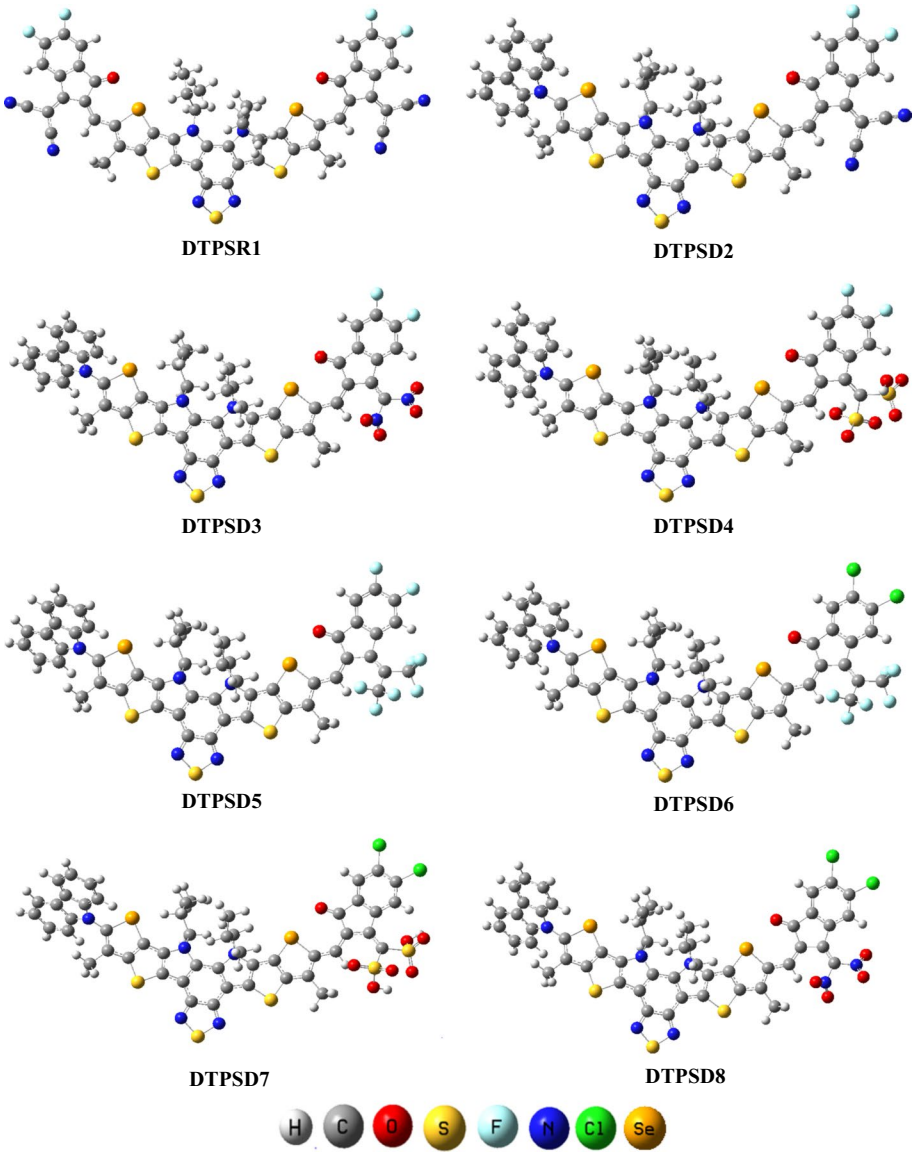

Fig. 1 Optimized structures of investigated compounds (**DTPSR1** and **DTPSD2**- **DTPSD8**)

with a smaller E_{LUMO}-E_{HOMO} energy gap are less stable, more reactive, soft, highly polarizable and are regarded as better entrants for estimating NLO response (Chattaraj and Roy 2007; Lesar and Milošev 2009; Parr et al. 1978; Parr, Szentpály and Liu 1999). DFT analysis for the estimation of E_{HOMO}, E_{LUMO}, and energy gaps of **DTPSR1** and **DTPS2-DTPSD8** is performed and the findings are tabulated in Table 1.

Originally, the reference molecule possessed an A–D–A architecture which is then modified to D–π–A for the exploration of effective NLO properties of newly designed compounds possessing various types of acceptor moieties. With new D–π–A architecture, the novel **DTPSD2**, **DTPSD3**, **DTPSD4** and **DTPSD7** compounds show almost similar results, which implies that the acceptors have a comparable influence on HOMO and LUMO energy gap of the molecules. Whereas, the highest energy gap value is observed in the case of **DTPSD5** and **DTPSD6**, respectively. The lowest value of energy gap of 3.53 eV is observed in the case of **DTPSD3** having (3-(dinitromethylene)-5,6-difluoro-2-methylene-2,3-dihydro-1*H*-inden-1-one) as acceptor group. This acceptor group showed remarkable effect on the UV–Vis absorption spectrum and comparable absorption spectra. This reduction in energy gap is due to the presence of strong electronegative nitro (–NO_2) and fluoro (–F) groups with greater negative inductive (−I) effect on the acceptor moiety. Similar energy gap of (3.53 eV) is also observed in the case of **DTPSD7** in which (5,6-dichloro-2-methylene-3-oxo-2,3-dihydro-1*H*-inden-1-ylidene)methanedisulfonic acid) group is used as acceptor moiety. This decline in energy gap is due to the existence of chloro (–Cl) and sulphonic acid (-SO_3H) groups on the acceptor part. As these groups have combined mesomeric and –I effect which results in decreased energy gap. Due to the use of most effective acceptor group in **DTPSD7**, the UV–Vis absorption spectra of respective molecule also correlate with this effective energy gap. The value of the energy gap is increased in case of **DTPSD8** (3.55 eV) having (5,6-dichloro-3-(dinitromethylene)-2-methylene-2,3-dihydro-1H-inden-1-one) as acceptor group. This enhancement in energy gap is due to the slightly less electron pulling nature of end-capped acceptor used in **DTPSD8** as a result of which the energy gap gets enhanced. This value of energy gap is further increased to (3.66 and 3.69 eV) for **DTPSD2** and **DTPSD4** possessing (2-(5,6-difluoro-2-methylene-3-oxo-2,3-dihydro-1*H*-inden-1-ylidene)malononitrile) and (5,6-difluoro-2-methylene-3-oxo-2,3-dihydro-1*H*-inden-1-ylidene)methanedisulfonic acid) groups as acceptor moieties, respectively. The energy gap of **DTPSD2** (3.66 eV) is less than **DTPSD4** (3.69 eV) because in **DTPSD2**, –F and –CN (both highly electron-withdrawing) are present, while in the case of **DTPSD4**, –F and **–**SO_3H (–F highly and **–**SO_3H moderately electron withdrawing) substituents are present on the acceptor unit. This value of energy gap with a slight

Table 1 The E_{HOMO}, E_{LUMO} and energy gap (E_{LUMO}-E_{HOMO}) of **DTPSR1** and **DTPSD2-DTPSD8**

Compounds	HOMO	LUMO	Δ*E*
DTPSR1	− 6.59	− 2.99	3.60
DTPSD2	− 6.50	− 2.83	3.66
DTPSD3	− 6.52	− 2.98	3.53
DTPSD4	− 6.52	− 2.83	3.69
DTPSD5	− 6.47	− 2.56	3.90
DTPSD6	− 6.48	− 2.63	3.85
DTPSD7	− 6.56	− 3.02	3.53
DTPSD8	− 6.531	− 2.98	3.55

Energy gap (ΔE) = $E_{LUMO} - E_{HOMO}$; Units in eV

increase (3.85 eV) is observed in the case of **DTPSD6** in which (5,6-dichloro-2-methylene-3-(perfluoropropan-2-ylidene)-2,3-dihydro-1*H*-inden-1-one) acceptor is used. Among all the designed compounds, the highest value of energy gap (3.90 eV) is noted in **DTPSD5** in which (5,6-difluoro-2-methylene-3-(perfluoropropan-2-ylidene)-2,3-dihydro-1*H*-inden-1-one) is used as acceptor moiety. The enhancement of energy gap of **DTPSD6** and **DTPSD5** is due to the presence of trifluoromethyl ($–CF_3$) group on the acceptor unit. As $–CF_3$ is highly electron-withdrawing group so, it strongly withdraws electron density towards itself and deactivate the ring by reducing resonance, hence, energy gap gets enhanced. Overall, the increasing order of energy gap in the newly modified reference and designed compounds is observed as: **DTPSD3 = DTPSD7 < DTPSD8 < DTPSR1 < DTPSD2 < DTPSD 4 < DTPSD6 < DTPSD5**.

The FMOs diagram indicating the presence and shifting of charge density from HOMO to LUMO is portrayed in Fig. 2. In reference compound **DTPSD1**, HOMO charge density from central core unit is shifted to terminal pulling units. The behavior of designed molecules is observed similar where HOMO is found populated on central units while LUMO is found concentrated on one side end-capped unit. The successful migration of charge density provide clue for potential enhancement in dipole moment which directly relate to the enhanced NLO response properties.

2.2 Global reactivity parameters (GRPs)

The FMO study ($E_{gap} = E_{LUMO}\text{-}E_{HOMO}$) is significant for evaluating the global reactivity parameters such as ionization potential (*IP*), global softness (σ), global hardness (η), global electrophilicity index (ω), electron affinity (*EA*), (Fukui 1982) electronegativity (*X*), and chemical potential (μ) (Chattaraj, Giri and Duley 2011; Kovačević and Kokalj 2011; Parr et al. 1978, 1999). The following Equations are used to calculate the *IP* and *EA*.

$$IP = -E_{HOMO} \tag{5}$$

$$EA = -E_{LUMO} \tag{6}$$

Applying Koopmans' theorem, the chemical hardness (η), chemical potential (μ), electronegativity (*X*), global softness (σ), and electrophilicity index (ω) were estimated (Kovačević and Kokalj 2011).

$$X = \frac{[IP + EA]}{2} \tag{7}$$

$$\eta = \frac{[IP - EA]}{2} \tag{8}$$

$$\mu = \frac{E_{HOMO} + E_{LUMO}}{2} \tag{9}$$

$$\sigma = \frac{1}{2\eta} \tag{10}$$

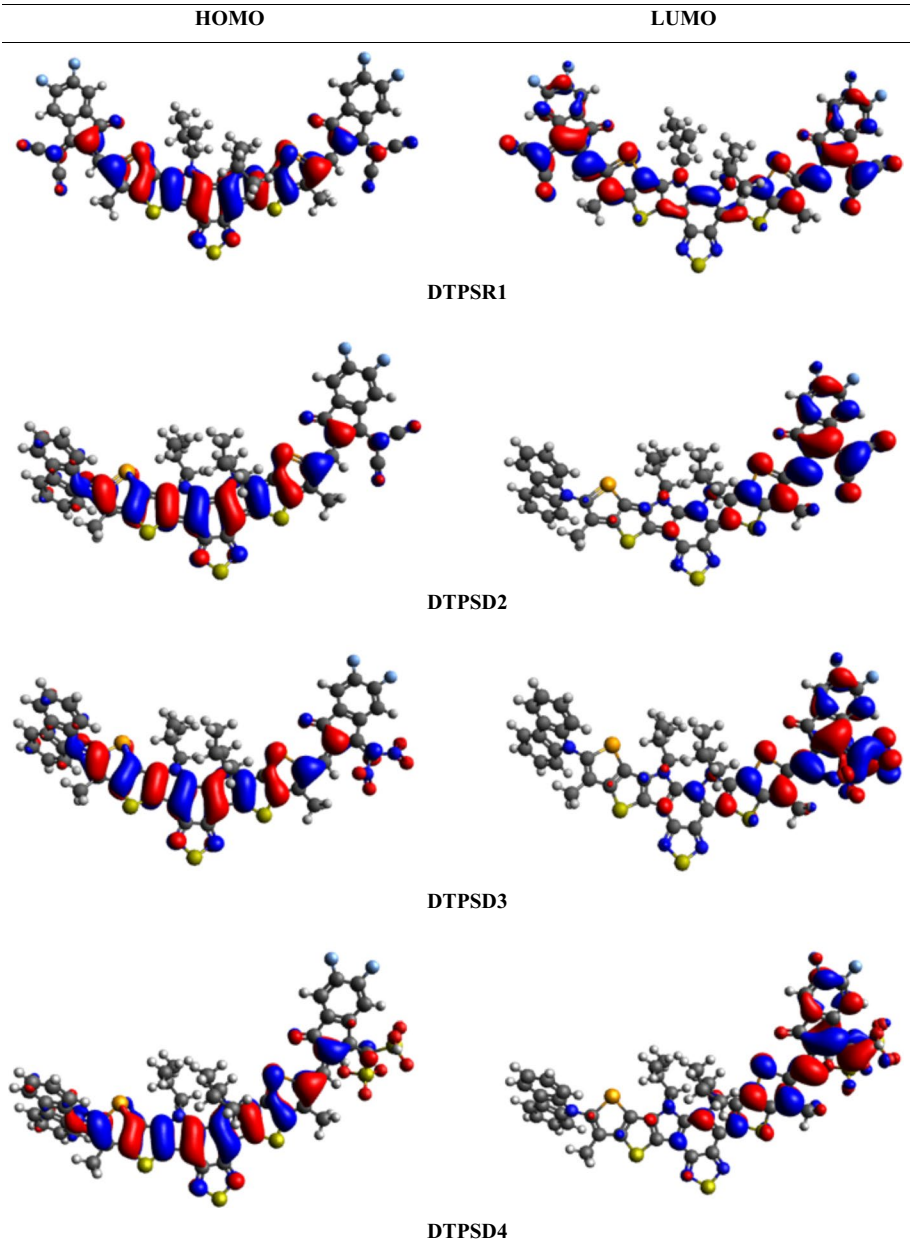

Fig. 2 HOMO and LUMO energy diagrams of studied compounds (**DTPSR1** and **DTPSD2**-**DTPSD8**)

$$\omega = \frac{\mu^2}{2\eta} \tag{11}$$

Ionization potential is the energy necessary to withdraw electron from HOMO which indicates the ability to accept electrons and affects the reactivity/stability of molecules

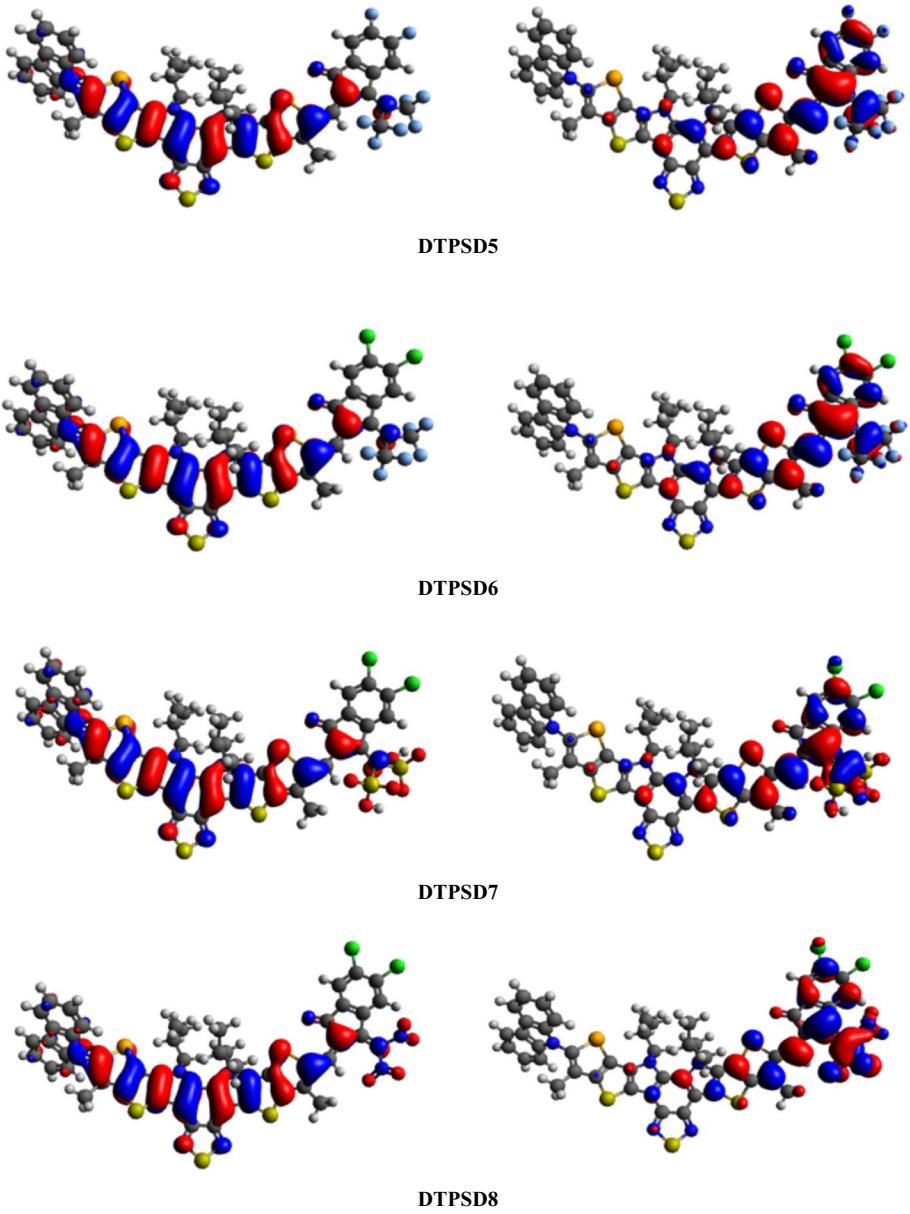

Fig. 2 (continued)

(Khalid et al. 2020a, b). The chemical potential, energy gap, hardness, and stability of a compound all are directly related while in case of reactivity the correlation is inversed (Khalid et al. 2020a, b). As a result, compounds with a greater energy gap generally considered as harder molecules, with less reactivity and high kinetic stability (Table 2).

The stability of a molecule is influenced by the location of electronegative substituents (He et al. 2010). **DTPSD3**, **DTPSD7** and **DTPSD8** have lower hardness as compared to

DTPSR1, whereas remaining all molecules depicts greater hardness than **DTPSR1**. The lowest computed hardness value is found 1.77 eV exhibited by **DTPSD7** which also show similar relationship with energy gap of the molecules. Overall, the increasing order of global hardness of **DTPSD2- DTPSD8** is marked as: **DTPSD3 = DTPSD7 = DTPSD8 < DTPSR1 < DTPSD2 < DTPSD4 < DTPSD6 < DTPSD5**. Softness is another parameter that reveals a molecule's reactivity because of its polarizability. In case of **DTPSD3**, **DTPSD7** and **DTPSD8**, the value of the global softness is enhanced (0.28 eV) so, they are considered as more polarizable units among other derivatives and consequently, they may hold proficient NLO behavior. The energy gap values of **DTPSD2-DTPSD8** are correlated with GRPs of the investigated compounds; compounds having smaller band gaps exhibited lesser hardness and larger softness along with lower chemical potential. It is evident from computed results that the investigated compounds hold proficient GRPs values essential to exhibit NLO response.

2.3 UV–Vis analysis

To explain the transitions and absorption attributes of **DTPSR1** and **DTPSD2- DTPSD8**, UV–Visible spectrum analysis is performed. The computations are conducted in dichloromethane (DCM) solvent. Through TD-DFT computations, six lowest singlet–singlet transitions have been explored. Transition energy (E eV), oscillator strength (f_{os}), transition nature and maximum absorbance wavelength (λ_{max}) are estimated and documented in Table S9. In Fig. 3, the absorbance spectra of **DTPSR1** and **DTPSD2- DTPSD8** are presented.

The computed λ_{max} of reference molecule **DTPSR1** is 583.592 nm, which is closer to the experimental value, and shows an absorption band in the range of 500–950 nm with two distinct bands at 760 and 660 nm (Lin et al. 2020). An effective chromophore would be capable to absorb a bulk of light in the visible spectrum (400–700 nm) (Liu et al. 2020). All the studied compounds depicted comparable results with respect to each other. Among all the designed molecules, **DTPSD7** shows the highest value of λ_{max} 586.269 nm with oscillation strength of 1.936. This absorption value is strongly supported by LUMO–HOMO energy gap value which is smallest among all the studied compounds. The lowest value of absorption is observed in the case of **DTPSD5** of 515.462 nm with corresponding oscillation strength of 1.893. This value is increased to 523.936 nm in case of **DTPSD6** having 1.943 oscillation strength. Furthermore, this value is enhanced to 551.408 and 553.427 nm with oscillation strength of 1.963

Table 2 Global reactivity parameters of studied compounds (**DTPSR1** and **DTPSD2-DTPSD8**)

Comps	*IP*	*EA*	*X*	η	μ	ω	σ
DTPSR1	6.59	2.99	4.79	1.80	−4.79	6.37	0.27
DTPSD2	6.50	2.84	4.67	1.83	−4.67	5.94	0.27
DTPSD3	6.53	2.98	4.76	1.77	−4.76	6.39	0.28
DTPSD4	6.52	2.82	4.68	1.85	−4.68	5.92	0.27
DTPSD5	6.48	2.57	4.52	1.95	−4.52	5.23	0.25
DTPSD6	6.49	2.63	4.56	1.93	−4.56	5.39	0.25
DTPSD7	6.57	3.03	4.79	1.77	−4.79	6.50	0.28
DTPSD8	6.53	2.98	4.75	1.77	−4.75	6.36	0.28

Units in eV

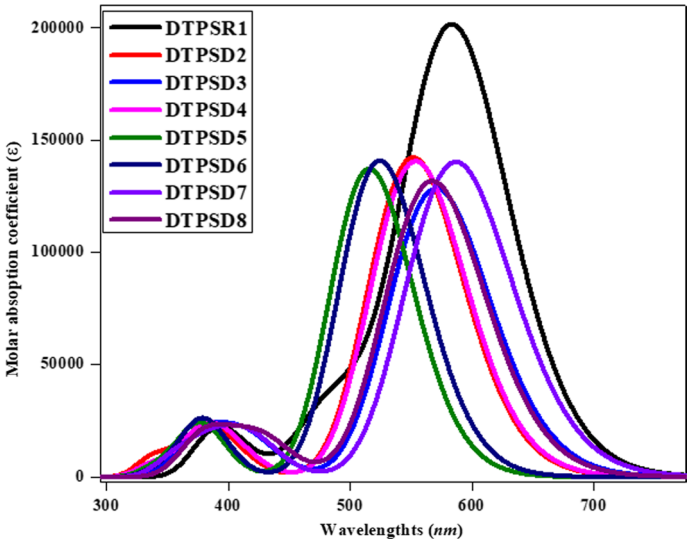

Fig. 3 Simulated absorption spectra of **DTPSR1** and **DTPSD2- DTPSD8**

and 1.941 in case of **DTPSD2** and **DTPSD4**, respectively. The λ_{max} value is further increased to 566.966 nm with corresponding oscillation strength of 1.819 in **DTPSD8**. This absorption value is further enhanced to 570.304 nm in **DTPSD3** with oscillation strength of 1.772. This efficient absorption followed by smallest band gap as evident of appropriate tailoring of D–π–A molecule, **DTPSD3**. Whereas, the highest absorbance value of 586.269 nm with oscillation strength of 1.936 is observed in **DTPSD7** which shows that **DTPSD7** have most effective acceptor moiety in D–π–A framework among the studied compounds. Overall, the ascending order of λ_{max} observed is as: **DTPSD5 < DTPSD6 < DTPSD2 < DTPSD4 < DTPSD8 < DTPSD3 < DTPSR1 < DTPSD7**. The absorption values of the **DTPSR1** and (**DTPSD2**-**DTPSD8**) are tabulated in Table S10 (Supplementary Information). The computed findings indicate that structural tailoring made a suitable impact on photophysical properties of the investigated compounds. Shifting of absorption value toward higher region, lowering of transition energy value in proposed compounds as compared to reference molecule advocate them better entrants for exhibiting fine NLO response.

2.4 Natural bond orbital (NBO) analysis

Natural bond orbital analysis is performed to investigate the interaction of bonds involving electron transmission and interpretation of hyper conjugation among the electrophile and nucleophile (Liu et al. 2020). The NBO analysis is helpful in the elucidation of uniform image formation of donor–π–acceptor framework, charge density shift from completely bonded to half-filled non-bonded NBO (Szafran et al. 2007). A second order perturbation approach is employed to compute delocalization reactions (Khalid et al. 2021a, b). The stabilizing energy $E^{(2)}$ aided with delocalization i → j, transition donor (i) and acceptor (j) is calculated by using the following Equation (Weinhold and Landis 2005).

$$E^{(2)} = q_i \frac{\left(F_{i,j}\right)^2}{\left(E_j - E_i\right)} \tag{12}$$

where $E^{(2)}$ determines the stabilization energy, F(i → j) depicts the diagonal, donor orbital occupancy is shown by q*i* and E_j,E_i are the off diagonal NBO Fock or Kohn–Sham medium components (Reed et al. 1988). When $E^{(2)}$ is large, i and j have a close correlation, and the total system has a higher degree of conjugation. The findings reveal that it is critical to create charge upon the carbon atom connected to the substituents by the donation and withdrawal of electrons. Introduction of highly electronegative nitro, fluoro and chloro groups enhance the conjugation and sustain the lone pair of atoms within the transition state (Khalid et al. 2021a, b). The computed interactions are tabulated in Table 3.

The analyzed compounds evince four important transitions such as π → π*, σ → σ*, LP → π* and LP → σ*. Wherein, foremost transitions were found to be π → π*, less prominent transitions are noted σ → σ* followed by slightly prominent transitions LP → π* and LP → σ*. The transfer of charge and hyper-conjugation of the studied compounds are detected via π → π* transitions. In the reference compound **DTPSR1**, the most prominent transition π(17-C18) → π*(C36-C37) with 39.33 kcal/mol energy is observed which indicates strong donor π acceptor π* interaction. Whereas, π(C58-O68) → π*(C36-C37) transition showed smallest stabilization energy of 4.06 kcal/mol. Similarly, transitions like σ(C36-H38) → σ*(C18-Se22) and σ(C70-N71) → σ*(C59-C69), respectively exhibited greatest and lowest value of stabilization energies 10.30 and 0.50 kcal/mol. These stabilization energy results are due to weak donor–acceptor interactions. In the case of resonance, the interaction LP1(N13) → π*(C3-C4) showed largest stabilization energy value of 47.60 kcal/mol and LP1(N7) → σ*(C1-C6) transition exhibited smallest energy value of 0.60 kcal/mol (see Table 3). Similarly, the transition π(C19-C24) → π*(C36-C37) with highest stabilization energy of 40.65 kcal/mol and π(C39-O49) → (C36-C37) with lowest energy value 4.05 kcal/mol are demonstrated by compound **DTPSD2**. Hence, σ(N8-S9) → σ*(C2-C3) and σ(C102-N103) → σ*(C40-C50) transitions in **DTPSD2** provides largest 9.31 kcal/mol and smallest 0.50 kcal/mol energy values, respectively. Due to the resonance, transitions such as LP1(N14) → π*(C5-C6) with stabilization energy 42.49 kcal/mol and LP1(N7) → σ*(C1-C6) having energy value 0.61 kcal/mol are manifested by compound **DTPSD2** as presented in Table 3. Similarly, the largest possible π → π* transition exist in **DTPSD3** is; π(C19-C24) → π*(C36-C37) with 41.44 kcal/mol value of stability. Moreover, the transition π(N100-O102) → π*(C40-C50) with least 0.68 kcal/mol stabilization energy value is displayed by **DTPSD3**. The highest and lowest stability values 10.13 and 0.50 kcal/mol with electronic transitions such as σ(C36-H38) → σ*(Se23-C24) and σ(C53-H55) → σ*(C53-C59) correspondingly are calculated because of weaker σ → σ* association. Additionally, LP3(O101) → π*(N100-O102) and LP1(N13) → σ*(C4-C5) transitions due to resonance with 223.99 and 0.50 kcal/mol stabilization energy are examined for **DTPSD3**. In **DTPSD4**, the most probable π → π* transition π(C19-C24) → π*(C36-C37) having stability energy of 42.71 kcal/mol is found. On the other hand, transition like π(C40-C50) → π*(C36-C37) with value 6.04 kcal/mol having lowest stabilization energy is observed. Furthermore, transition σ(C36-H38) → σ*(Se23-C24) shows prominent energy value of 10.36 kcal/mol, whereas, σ(C56-H57) → σ*(C69-H70) transition with least stabilization energy value of 0.50 kcal/mol is examined. However due to resonance phenomena, the largest 43.01 kcal/mol and smallest 1.84 kcal/mol energy values are exhibited by LP1(N14) → π*(C5-C6) and LP1(Se22) → σ*(C16-C25) transitions correspondingly. The π(C19-C24) → π*(C36-C37) transition is detected with highest energy value 37.44 kcal/

Table 3 Second order perturbation theory analysis of Fock matrix NBO at M06-2X/6-311G(d,p) level for **DTPSR1** and **DTPSD2**-**DTPSD8**

Comps	Donor(i)	Type	Acceptor(j)	Type	E(2)[a]	E(J)E(i)[b]	F(i,j)[c]
DTPSR1	C17-C18	π	C36-C37	π*	39.33	0.37	0.109
	C58-O68	π	C36-C37	π*	4.06	0.52	0.044
	C36-H38	σ	C18-Se22	σ*	10.30	0.77	0.080
	C70-N71	σ	C59-C69	σ*	0.50	1.82	0.027
	N13	LP(1)	C3-C4	π*	47.60	0.36	0.119
	N7	LP(1)	C1-C6	σ*	0.60	1.08	0.023
DTPSD2	C19-C24	π	C36-C37	π*	40.65	0.37	0.111
	C39-O49	π	C36-C37	π*	4.05	0.52	0.044
	N8-S9	σ	C2-C3	σ*	9.31	1.38	0.102
	C102-N103	σ	C40-C50	σ*	0.50	1.82	0.027
	N14	LP(1)	C5-C6	π*	42.49	0.37	0.115
	N7	LP(1)	C1-C6	σ*	0.61	1.08	0.023
DTPSD3	C19-C24	π	C36-C37	π*	41.44	0.37	0.111
	N100-O102	π	C40-C50	π*	0.68	0.61	0.019
	C36-H38	σ	Se23-C24	σ*	10.13	0.77	0.079
	C53-H55	σ	C53-C59	σ*	0.50	1.01	0.020
	O101	LP(3)	N100-O102	π*	223.99	0.22	0.197
	N13	LP(1)	C4-C5	σ*	0.50	0.93	0.021
DTPSD4	C19-C24	π	C36-C37	π*	42.71	0.37	0.113
	C40-C50	π	C36-C37	π*	6.04	0.44	0.048
	C36-H38	σ	Se23-C24	σ*	10.36	0.77	0.080
	C56-H57	σ	C69-H70	σ*	0.50	1.09	0.021
	N14	LP(1)	C5-C6	π*	43.01	0.37	0.115
	Se22	LP(1)	C16-C25	σ*	1.84	1.39	0.045
DTPSD5	C19-C24	π	C36-C37	π*	37.44	0.38	0.108
	C39-O49	π	C36-C37	π*	3.96	0.53	0.043
	C20-C21	σ	N14-C15	σ*	10.02	1.29	0.102
	C28-H29	σ	C19-C28	σ*	0.50	1.04	0.020
	N14	LP(1)	C5-C6	π*	43.23	0.37	0.115
	N14	LP(1)	C12-C15	σ*	0.59	0.92	0.023
DTPSD6	C5-C6	π	C1-N7	π*	30.76	0.34	0.093
	C39-O49	π	C36-C37	π*	3.95	0.52	0.043
	C20-C21	σ	N14-C15	σ*	10.04	1.29	0.102
	C51-H53	σ	C51-C57	σ*	0.50	1.01	0.020
	N14	LP(1)	C5-C6	π*	43.46	0.37	0.116
	F105	LP(1)	C50-C98	σ*	0.51	1.60	0.026
DTPSD7	C19-C24	π	C36-C37	π*	46.16	0.37	0.117
	C39-O49	π	C36-C37	π*	3.70	0.52	0.042
	C36-H38	σ	Se23-C24	σ*	10.31	0.77	0.079
	C51-H53	σ	C51-C57	σ*	0.50	1.01	0.020
	N14	LP(1)	C5-C6	π*	43.94	0.37	0.116
	Cl99	LP(2)	C43-C44	σ*	0.53	0.99	0.020
	C19-C24	π	C36-C37	π*	42.36	0.37	0.113
	C40-C50	π	N103-O104	π*	1.21	0.26	0.018

Table 3 (continued)

Comps	Donor(i)	Type	Acceptor(j)	Type	E(2)[a]	E(J)E(i)[b]	F(i,j)[c]
DTPSD8	C20-C21	σ	N14-C15	σ*	10.13	1.29	0.102
	C51-H53	σ	C51-C57	σ*	0.50	1.01	0.02
	O105	LP(3)	N103-O104	π*	228.91	0.21	0.198
	Se23	LP(1)	C39-O49	σ*	0.50	1.45	0.024

[a] $E^{(2)}$ means the stabilization energy in kcal/mol

[b] Energy difference between donor (i) and acceptor (j) NBO orbitals

[c] F(i;j) is the Fock matrix element between donor and acceptor orbitals

mol in compound **DTPSD5**. Whereas, π(C39-O49) → π*(C36-C37) transition is observed with stabilization energy value of 3.96 kcal/mol expressing least stability value. In addition to this, maximum and minimum energy values 10.02 and 0.50 kcal/mol are noticed because of σ(C20-C21) → σ*(N14-C15) and σ(C28-H29) → σ*(C19-C28) transitions, respectively. Furthermore, transitions LP1(N14) → π*(C5-C6) and LP1(N14) → σ*(C12-C15) with dominant and least stabilization energies to be 43.23 and 0.59 kcal/mol are observed. The compound **DTPSD6** manifested the transition π(C5-C6) → π*(C1-N7) with greatest energy value 30.76 kcal/mol and π(C39-O49) → π*(C36-C37) exhibited lowest stability value of 3.95 kcal/mol. However, largest stabilization energy value 10.04 kcal/mol is shown by σ(C20-C21) → σ*(N14-C15) transition while least stability value 0.50 kcal/mol is displayed by σ(C51-H53) → σ*(C51-C57) transition due to weak σ → σ* association. Whiledue to resonance phenomena, maximum and minimum stabilization energies of 43.46 and 0.51 kcal/mol are presented by LP1(N14) → π*(C5-C6) and LP1(F105) → σ*(C50-C98) electronic transitions. For **DTPSD7**, the transition π(C19-C24) → π*(C36-C37) with greatest stabilization energy value 46.16 kcal/mol while π(C39-O49) → π*(C36-C37) with lowest stabilization energy value 3.70 kcal/mol are observed. The transitions σ(C36-H38) → σ*(Se23-C24) and σ(C51-H53) → σ*(C51-C57) having 10.31 and 0.50 kcal/mol energies are noted. The highest and lowest stabilization energies 43.94 and 0.53 kcal/mol are demonstrated by LP1(N14) → π*(C5-C6) and LP2(Cl99) → σ*(C43-C44) transitions, respectively. In **DTPSD8**, the transition π(C19-C24) → π*(C36-C37) with greatest stabilization energy of 42.36 kcal/mol is calculated. Whereas, π(C40-C50) → π*(N103-O104) with lowermost stabilization energy value 1.21 kcal/mol is calculated. The transitions such as σ(C20-C21) → σ*(N14-C15) and σ(C51-H53) → σ*(C51-C57) having 10.13 and 0.50 kcal/mol energies are illustrated. LP3(O105) → π*(N103-O104) and LP1(Se23) → σ*(C39-O49) transitions are obtained with stability energy of 228.91 and 0.50 kcal/mol due to resonance. Several additional conjugation-exhibiting transitions are also explored in **DTPSR1** and **DTPSD2-DTPSD8** which are represented in Tables S2-S9 (Supplementary Information). Amongst all investigated chromophores, **DTPSD7** has the superior stability because of the existence of comprehensive conjugation with 46.16 kcal/mol energy. In comparison with the **DTPSR1**, except **DTPSD5** and **DTPSD6**, all the designed chromophores disclosed greater stability. The general ascending arrangement of stability is represented as: **DTPSD6 < DTPSD5 < DTPSR1 < DTPSD2 < DTPSD3 < DTPSD8 < DTPSD4 < DTPSD7**. Hence, NBO study implies that the extended hyper-conjugation and vigorous ICT plays a marvelous role in stabilization of these compounds and designate the charge transference characteristics that are crucial for NLO response.

2.5 Nonlinear optical (NLO) properties

The significance of NLO materials is acknowledged due to its implications in medical, electronics, optical transmission modulation, and telecom (Muhammad et al. 2009, 2013). Organic compounds have significantly greater ability to display strong NLO abilities than inorganic molecules (Bi et al. 2008). Asymmetric polarizability generates the NLO response in organic molecules. The presence of electron-withdrawing and electron-donating moieties within the molecules at appropriate positions provides significant push–pull architecture, which may generate the superior NLO response. Furthermore, these electron-withdrawing and electron-donating groups are linked to the π-conjugated linker which enhances the NLO behavior. As per literature, the energy gap among LUMO and HOMO has impact on polarizability of molecules. High hyperpolarizability and linear polarizability values are found in compounds with a smaller energy gap (Qin and Clark 2007). As a consequence, dipole polarizabilities and ICT are a quantitative evaluation which offers insights into the exceptional NLO activity of non-fullerene based compounds. Table 4 illustrates the calculated results whereas; Table S19-S21 (Supplementary Information) presents the major contributing tensor values.

Among all the molecules, **DTPSD4** has the maximum dipole moment of 4.78 *D*, while **DTPSD5** have shown the minimum dipole moment of 2.35 *D*. Furthermore, while comparing to the urea as a standard molecule (1.3732 *D*), the dipole moments of all tailored molecules are observed to be higher (Reis et al. 1998) than the reference molecule (**DTPSR1**). The **DTPSD4** has higher polarizability and hyperpolarizability, with amplitudes 1350.53 and 153,255.97 a.u. Moreover, the linear polarizability variable is a significant factor in determining the electrical characteristics of organic molecules. The linear polarizability values for **DTPSR1** are reported to be 2681.96, 1521.55, and 488.05 a.u. along a_{xx}, a_{yy}, and a_{zz} axes, respectively (Table S19). The linear polarizability values of all the designed compounds are ranging from (1244.99–1439.16 a.u.). Among all the derivatives, **DTPSD7** has the highest linear polarizability 1439.16 a.u. The average polarizability in ascending order is noted as: **DTPSD5 < DTPSD6 < DTPSD2 < DTPSD3 < DTPSD4 < DTPSD8 < DTPSD7 < DTPSR1**. Among all the designed compounds, the highest value 189,720.55 a.u. of β_{total} is noted in case of **DTPSD7** in which (5,6-dichloro-2-methylene-3-oxo-2,3-dihydro-1*H*-inden-1-ylidene)methanedisulfonic acid) group is used as an acceptor group. This hyperpolarizability reduced to 179,804.05 a.u. in **DTPSD3** in which (3-(dinitromethylene)-5,6-difluoro-2-methylene-2,3-dihydro-1*H*-inden-1-one) acceptor group is used. Whereas, the lowest value 104,707.22 a.u. of β_{total} is observed for **DTPSD5**. All the designed

Table 4 The computed dipole moment (μ), linear polarizability $\langle\alpha\rangle$, first-order hyperpolarizability (β_{total}) and second-order hyper polarizability (γ_{total}) of entitled compounds (**DTPSR1**and **DTPSD2–DTPSD8**)

Comp	μ_{total}	$\langle\alpha\rangle$	β_{total}	$\gamma_{total}\times10^{7}$
DTPSR1	1.95	1563.85	80,048.09	3.30
DTPSD2	3.92	1324.37	161,420.17	1.73
DTPSD3	3.86	1324.96	179,804.05	2.04
DTPSD4	4.78	1350.53	153,255.97	1.96
DTPSD5	2.36	1244.99	104,707.22	1.10
DTPSD6	2.46	1298.39	115,489.55	1.23
DTPSD7	4.57	1439.16	189,720.55	1.98
DTPSD8	4.68	1370.25	170,314.05	1.87

Units in a.u

compounds (**DTPSD2**- **DTPSD8**) depict greater value of β_{total} than the reference compound (**DTPSR1**) which indicates that these compounds may have excellent NLO behavior. It can be correlated with the dipole moments of **DTPSD2-DTPSD8** which is greater than that of **DTPSR1**. Overall, the increasing order of β_{total} values is measured as: **DTPSR 1 < DTPSD5 < DTPSD6 < DTPSD4 < DTPSD2 < DTPSD8 < DTPSD3 < DTPSD7**.

For NLO compounds, the second-order hyperpolarizability (γ_{total}) is also significant and the γ_{total} of **DTPSR1** is 3.30×10^7 a.u. with tensor values 3.29×10^7, 1.73×10^5 and 7.58×10^4 a.u. along the γ_{xx}, γ_{yy}, and γ_{zz} axes, respectively. The highest γ_{total} 2.04×10^7 a.u. is observed for **DTPSD3** with γ_{xx}, γ_{yy}, and γ_{zz} tensors values of 1.95×10^7, 7.37×10^5 and 6.98×10^4 a.u., correspondingly among all the analyzed molecules. **DTPSD5** has the lowest γ_{total} value1.10×10^7 a.u. with tensor values of 1.10×10^7, 6.97×10^5 and 6.07×10^4 a.u., accordingly along γ_{xx}, γ_{yy}, and γ_{zz} axes. The values of γ_{total} in ascending order are as: **DT PSD5 < DTPSD6 < DTPSD2 < DTPSD8 < DTPSD4 < DTPSD7 < DTPSD3 < DTPSR1**. Table S21(Supplementary Information) provides all the tensor values of γ_{total} for all the molecules (**DTPSR1** and **DTPSD2-DTPSD8**). The energy gap influences polarizability and explore the significant NLO responses, a shorter energy gap and higher polarizability are connected with larger hyperpolarizabilities (Khalid et al. 2020a, b). Hence, the energy gap and NLO responses are found to be inversely related with each other in studied molecules. All NLO computed results conclude that investigated molecules have proficient NLO features and can be used as fine entrants for future NLO applications.

2.6 Transition density matrix (TDM)

Transition density matrix (TDM) analysis is used to determine the nature of transition in **DTPSR1** and **DTPSD2**- **DTPSD8**. It also helps to understand the behavior of transitions, from the ground state (S_0) to an excited state (S_1) and interaction between acceptor and donor moieties (Ans et al. 2018). The compounds are divided into three fragments such as terminal donor, central core π-spacer and peripheral acceptor represented as D–π–A network and their heat maps are shown in Fig. 4.

FMOs study reveals the charge transfer that occurs majorly on the central π-spacer and minutely on the peripheral acceptor and donor moieties which brings remarkable changes in TDM pictographs. From TDM heat maps, it is clear that in all the derivatives, charge is diagonally transferred from central core π-spacer to end capped acceptor and then to peripheral donor part.

Binding energy is another interesting feature for analyzing the optoelectronic properties of investigated compounds. It assists in the understanding of excitation dissociation potential. In the higher energy state, the lower the binding energy, the stronger the excitation dissociation.

$$E_b = E_{L-H} - E_{opt} \tag{13}$$

The difference between the LUMO–HOMO (E_{gap}) is the smallest for first activation energy that can be used to determine binding energy E_b. The E_{opt} is a term refers to the potential of first singlet excited state that varies from S0 to S1. In Eq. (13), E_b is the binding energy, $E_{H\text{-}L}$ is the energy gap and the first excitation energy is $E_{opt.}$ (Khalid et al. 2021a, b). Table 5 shows the theoretically calculated binding energies of investigated compounds.

Where E_H is the energy of highest occupied molecular orbital (HOMO) and E_L is the energy of the lowest unoccupied molecular orbital (LUMO). The increasing order of binding energies is computed in this order: **DTPSD3** (1.36) < **DTPSD8** (1.37) < **DTPSD2**

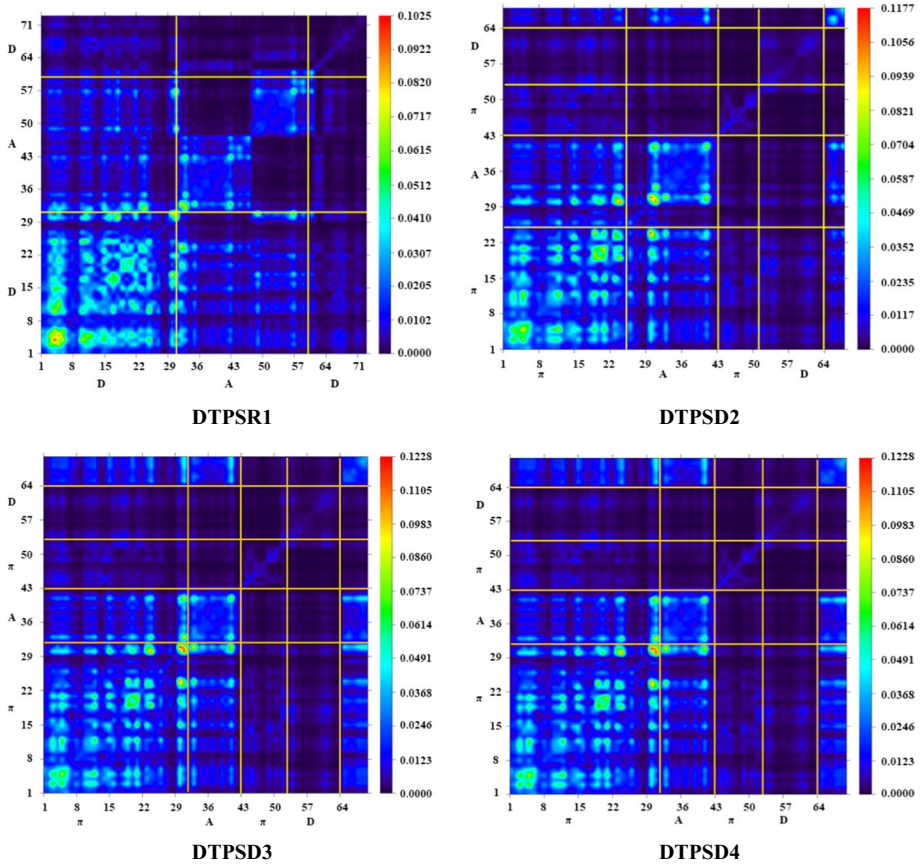

Fig. 4 TDM graphs of compounds (**DTPSR1** and **DTPSD2**-**DTPSD8**)

(1.41) < **DTPSD7** (1.42) < **DTPSD4** (1.45) < **DTPSD6** (1.48) = **DTPSR1** (1.48) < **DTPSD5** (1.49) eV which is quite comparable to the TDM pictographs. All designed compounds possess almost comparable E_b except **DTPSD3** which shows smallest E_b value of 1.36 eV that predicts superior optoelectronic properties with greater magnitude of excitation in excited state. In comparison to the reference compound **DTPSR1**, all designed chromophores except **DTPSD6** have reduced binding energies that results in more excitation dissociation in the higher energy state. Thus, newly designed compounds may have promising optical activity and might be utilized in various NLO applications.

3 Conclusion

A series of non-fullerene based organic compounds (**DTPSR1** and **DTPSD2**-**DTPSD8**) having D–π–A configuration was successfully designed by the structural modification with different end capped acceptor units. It was observed that different acceptors have significant impact on D–π–A arrangement and enhanced the NLO properties of designed chromophores. It was observed that among all the designed derivatives, **DTPSD7** displayed

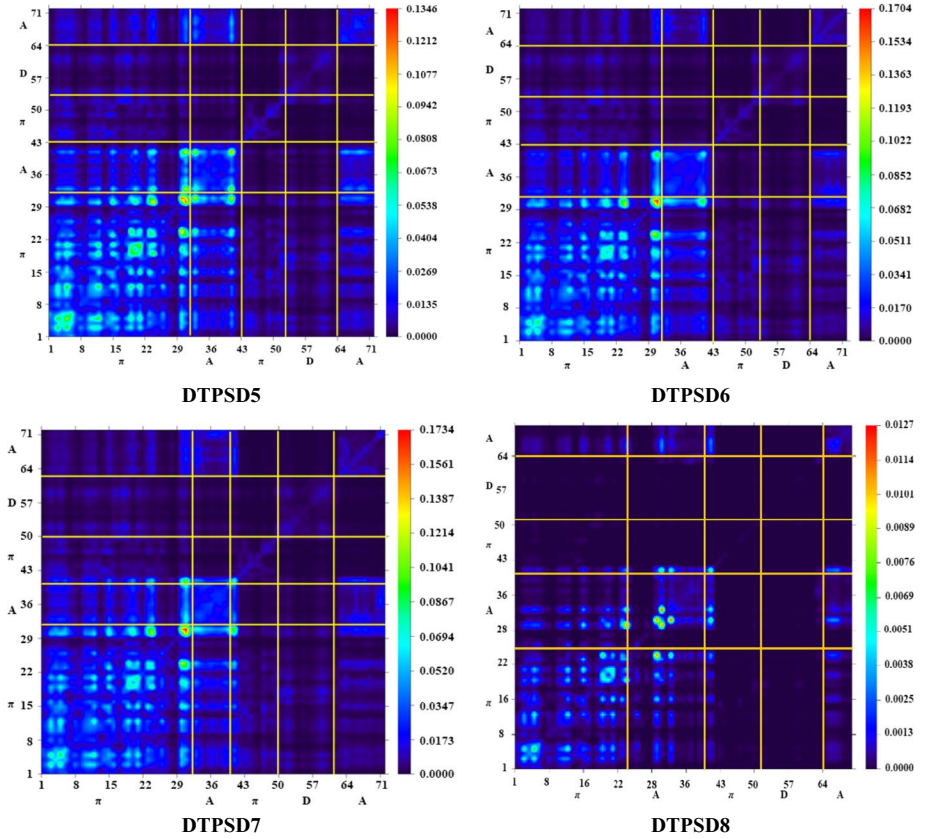

Fig. 4 (continued)

Table 5 Calculated LUMO–HOMO energy gap ($E_{L\text{-}H}$), first singlet excitation energies (E_{opt}), and excitation binding energies (E_b) of investigated compounds (**DTPSR1** and **DTPSD2-DTPSD8**)

Comp	$E_{L\text{-}H}$	E_{opt}	E_b
DTPSR1	3.60	2.12	1.48
DTPSD2	3.66	2.25	1.41
DTPSD3	3.53	2.17	1.36
DTPSD4	3.69	2.24	1.45
DTPSD5	3.90	2.41	1.49
DTPSD6	3.85	2.37	1.48
DTPSD7	3.53	2.11	1.42
DTPSD8	3.55	2.18	1.37

Units in eV

maximum red shift of $\lambda_{max} = 586.27$ nm and lowest transition energy 1.94 eV. FMOs study indicates that LUMO–HOMO energy gap of **DTPSD2-DTPSD8** lies in the range of 3.53–3.90 eV. Additionally, GRPs data estimated that **DTPSD3**, **DTPSD7** and **DTPSD8** exhibited greater value of softness (0.28 eV) as compared to **DTPSR1** (**0.27** eV) NBO findings revealed the charge transfer improves the stability of all designed compounds

except **DTPSD5** and **DTPSD6** which was further supported by GRPs outcomes. **DTPSD7** exhibited excellent NLO response through highest values of $\langle\alpha\rangle$, β_{total} and γ_{total} computed to be 1439.16, 189,720.55 and 1.98×10^{7} a.u., respectively. The dipole polarizability trend confirms that all the designed compounds have polar characteristics. The current study also yields insights that successful π-conjugated push–pull phenomenon can takes place in investigated designed chromophores to render promising NLO results and can be utilized in modern NLO applications.

Supplementary Information The online version contains supplementary material available at https://doi.org/10.1007/s11082-022-04441-w.

Acknowledgements Dr. Muhammad Khalid gratefully acknowledges the financial support of HEC Pakistan (project no. 20-14703/NRPU/R&D/HEC/2021). Authors are also thankful for cooperation and collaboration of A.A.C.B from IQ-USP, Brazil especially for his continuous support and providing computational lab facilities. S.F.A.M. acknowledges CNPq for the scholarship (Grant 165726/2020-2). A.A.C.B. (grants 2011/07895-8, 2015/01491-3, and 2014/25770-6) is highly thankful to Fundação de Amparo à Pesquisa do Estado de São Paulo for the cooperation and financial assistance. A.A.C.B. (grant 312550/2020-0) also thanks to the Brazilian National Research Council (CNPq) for financial support and fellowships.

Author contributions MK: Methodology; software; project administration; SN: Data curation; formal analysis; MST: Resources; software; supervision; IS: Data curation; formal analysis; KSM: Conceptualization; resources; SFAM: Conceptualization; methodology; AACB: Data curation; formal analysis; validation.

Funding The authors have not disclosed any funding.

Declarations

Conflict of interest The authors declare no competing interests.

References

Ahmad, M.S., Khalid, M., Shaheen, M.A., Tahir, M.N., Khan, M.U., Braga, A.A.C., Shad, H.A.: Synthesis and XRD, FT-IR vibrational, UV–vis, and nonlinear optical exploration of novel tetra substituted imidazole derivatives: A synergistic experimental-computational analysis. J. Phys. Chem. Solids **115**, 265–276 (2018)

Akram, M., Adeel, M., Khalid, M., Tahir, M.N., Khan, M.U., Asghar, M.A., Ullah, M.A., Iqbal, M.: A combined experimental and computational study of 3-bromo-5-(2, 5-difluorophenyl) pyridine and 3, 5-bis (naphthalen-1-yl) pyridine: Insight into the synthesis, spectroscopic, single crystal XRD, electronic, nonlinear optical and biological properties. J. Mol. Struct. **1160**, 129–141 (2018)

Amiri, S.S., Makarem, S., Ahmar, H., Ashenagar, S.: Theoretical studies and spectroscopic characterization of novel 4-methyl-5-((5-phenyl-1, 3, 4-oxadiazol-2-yl) thio) benzene-1, 2-diol. J. Mol. Struct. **1119**, 18–24 (2016)

Ans, M., Iqbal, J., Ahmad, Z., Muhammad, S., Hussain, R., Eliasson, B., Ayub, K.: Designing three-dimensional (3D) non-fullerene small molecule acceptors with efficient photovoltaic parameters. ChemistrySelect **3**(45), 12797–12804 (2018)

Barone, V., Cossi, M.: Quantum calculation of molecular energies and energy gradients in solution by a conductor solvent model. J. Phys. Chem. A **102**(11), 1995–2001 (1998)

Bi, W., Louvain, N., Mercier, N., Luc, J., Rau, I., Kajzar, F., Sahraoui, B.: A switchable NLO organic-inorganic compound based on conformationally chiral disulfide molecules and Bi (III) I5 iodobismuthate networks. Adv. Mater. **20**(5), 1013–1017 (2008)

Breitung, E.M., Shu, C.-F., McMahon, R.J.: Thiazole and thiophene analogues of donor− acceptor stilbenes: molecular hyperpolarizabilities and structure− property relationships. J. Am. Chem. Soc. **122**(6), 1154–1160 (2000)

Chattaraj, P.K., Roy, D.R.: Update 1 of: electrophilicity index. Chem. Rev. **107**(9), PR46–PR74 (2007)

Chattaraj, P., Giri, S., Duley, S.: Update 2 of: electrophilicity index. Chem. Rev. **111**(2), PR43–PR75 (2011)

Chemla, D.S.: Nonlinear Optical Properties of Organic Molecules and Crystals V1, vol. 1. Elsevier (2012)

Cheng, P., Li, G., Zhan, X., Yang, Y.: Next-generation organic photovoltaics based on non-fullerene acceptors. Nat. Photonics **12**(3), 131–142 (2018)

Dennington, R., Keith, T.A., Millam, J.M.: GaussView 6.0. 16. Semichem Inc. (2016)

Eaton, D.F.: Nonlinear Optical Materials: The Great and Near Great. ACS Publications (1991)

Fonseca, R.D., Vivas, M.G., Silva, D.L., Eucat, G., Bretonnière, Y., Andraud, C., De Boni, L., Mendonca, C.R.: First-order hyperpolarizability of triphenylamine derivatives containing cyanopyridine: molecular branching effect. J. Phys. Chem. C **122**(3), 1770–1778 (2018)

Frisch, M., Clemente, F.: Gaussian 09, revision a. 01, mj frisch, gw trucks, hb schlegel, ge scuseria, ma robb, jr cheeseman, g. *Scalmani, V. Barone, B. Mennucci, GA Petersson, H. Nakatsuji, M. Caricato, X. Li, HP Hratchian, AF Izmaylov, J. Bloino, G. Zhe*, pp. 20–44 (2009)

Fukui, K.: Role of frontier orbitals in chemical reactions. Science **218**(4574), 747–754 (1982)

Glendening, E.D., Weinhold, F.: Natural resonance theory: I. General formalism. J. Comput. Chem. **19**(6), 593–609 (1998)

Gunasekaran, S., Balaji, R.A., Kumeresan, S., Anand, G., Srinivasan, S.: Experimental and theoretical investigations of spectroscopic properties of N-acetyl-5-methoxytryptamine. Can. J. Anal. Sci. Spectrosc. **53**(4), 149–162 (2008)

Guo, L., Guo, Z., Li, X.: Design and preparation of side chain electro-optic polymeric materials based on novel organic second order nonlinear optical chromophores with double carboxyl groups. J. Mater. Sci. Mater. Electron. **29**(3), 2577–2584 (2018)

Halasyamani, P.S., Zhang, W.: Inorganic Materials for UV and Deep-UV Nonlinear-Optical Applications, vol. 56, pp. 12077–12085. ACS Publications (2017)

Hanwell, M.D., Curtis, D.E., Lonie, D.C., Vandermeersch, T., Zurek, E., Hutchison, G.R.: Avogadro: an advanced semantic chemical editor, visualization, and analysis platform. J Cheminformatics **4**(1), 1–17 (2012)

Haroon, M., Mahmood, R., Janjua, M.R.S.A.: An Interesting behavior and nonlinear optical (NLO) response of hexamolybdate metal cluster: theoretical insight into electro-optic modulation of hybrid composites. J. Cluster Sci. **28**(5), 2693–2708 (2017)

He, Y., Li, Y.: Fullerene derivative acceptors for high performance polymer solar cells. Phys. Chem. Chem. Phys. **13**(6), 1970–1983 (2011)

He, S., Tan, Y., Xiao, X., Zhu, L., Guo, Y., Li, M., Tian, A., Pu, X., Wong, N.-B.: Substituent effects on electronic character of the CN group and trans/cis isomerization in the C-substituted imine derivatives: a computational study. J. Mol. Struct. Thoechem. **951**(1–3), 7–13 (2010)

Janjua, M.R.S.A.: Quantum mechanical design of efficient second-order nonlinear optical materials based on heteroaromatic imido-substituted hexamolybdates: first theoretical framework of POM-based heterocyclic aromatic rings. Inorg. Chem. **51**(21), 11306–11314 (2012)

Janjua, M.R.S.A., Su, Z.-M., Guan, W., Liu, C.-G., Yan, L.-K., Song, P., Maheen, G.: Tuning second-order non-linear (NLO) optical response of organoimido-substituted hexamolybdates through halogens: Quantum design of novel organic-inorganic hybrid NLO materials. Aust. J. Chem. **63**(5), 836–844 (2010)

Janjua, M.R.S.A., Khan, M.U., Bashir, B., Iqbal, M.A., Song, Y., Naqvi, S.A.R., Khan, Z.A.: Effect of π-conjugation spacer (CC) on the first hyperpolarizabilities of polymeric chain containing polyoxometalate cluster as a side-chain pendant: a DFT study. Comput. Theor. Chem. **994**, 34–40 (2012b)

Janjua, M.R.S.A., Jamil, S., Ahmad, T., Yang, Z., Mahmood, A., Pan, S.: Quantum chemical perspective of efficient NLO materials based on dipolar trans-tetraammineruthenium (II) complexes with pyridinium and thiocyanate ligands: first theoretical framework. Comput. Theor. Chem. **1033**, 6–13 (2014)

Janjua, M.R.S.A., Jamil, S., Mahmood, A., Zafar, A., Haroon, M., Bhatti, H.N.: Solvent-dependent nonlinear optical properties of 5, 5′-disubstituted-2, 2′-bipyridine complexes of ruthenium (II): a quantum chemical perspective. Aust. J. Chem. **68**(10), 1502–1507 (2015a)

Janjua, M.R.S.A., Yamani, Z.H., Jamil, S., Mahmood, A., Ahmad, I., Haroon, M., Tahir, M.H., Yang, Z., Pan, S.: First principle study of electronic and non-linear optical (NLO) properties of triphenylamine dyes: interactive design computation of new NLO compounds. Aust. J. Chem. **69**(4), 467–472 (2015b)

Janjua, M. R. S. A., Amin, M., Ali, M., Bashir, B., Khan, M. U., Iqbal, M. A., Guan, W., Yan, L., Su, Z. M.: A DFT study on the two-dimensional second-order nonlinear optical (NLO) response of terpyridine-substituted hexamolybdates: physical insight on 2D inorganic–organic hybrid functional materials (2012a)

Katono, M., Wielopolski, M., Marszalek, M., Bessho, T., Moser, J.-E., Humphry-Baker, R., Zakeeruddin, S.M., Grätzel, M.: Effect of extended π-conjugation of the donor structure of organic D-A− π–A dyes on the photovoltaic performance of dye-Sensitized solar cells. J. Phys. Chem. C **118**(30), 16486–16493 (2014)

Khalid, M., Ali, M., Aslam, M., Sumrra, S.H., Khan, M.U., Raza, N., Kumar, N., Imran, M.: Frontier molecular, Natural bond orbital, UV-Vis spectral stduy, Solvent influence on geometric parameters, Vibrational frequencies and solvation energies of 8-Hydroxyquinoline. Int. J. Pharm. Sci. Res. **8**(2), 457–469 (2017)

Khalid, M., Ali, A., Jawaria, R., Asghar, M.A., Asim, S., Khan, M.U., Hussain, R., ur Rehman, M.F., Ennis, C.J., Akram, M.S.: First principles study of electronic and nonlinear optical properties of A-D–π–A and D-A–D–π–A configured compounds containing novel quinoline–carbazole derivatives. RSC Adv. **10**(37), 22273–22283 (2020a)

Khalid, M., Ali, A., Rehman, M.F.U., Mustaqeem, M., Ali, S., Khan, M.U., Asim, S., Ahmad, N., Saleem, M.: Exploration of noncovalent interactions, chemical reactivity, and nonlinear optical properties of piperidone derivatives: a concise theoretical approach. ACS Omega **5**(22), 13236–13249 (2020b)

Khalid, M., Khan, M.U., Razia, E.-T., Shafiq, Z., Alam, M.M., Imran, M., Akram, M.S.: Exploration of efficient electron acceptors for organic solar cells: rational design of indacenodithiophene based non-fullerene compounds. Sci. Rep. **11**(1), 1–15 (2021a)

Khalid, M., Lodhi, H.M., Khan, M.U., Imran, M.: Structural parameter-modulated nonlinear optical amplitude of acceptor–π–D–π–donor-configured pyrene derivatives: a DFT approach. RSC Adv. **11**(23), 14237–14250 (2021b)

Khan, M.U., Khalid, M., Ibrahim, M., Braga, A.A.C., Safdar, M., Al-Saadi, A.A., Janjua, M.R.S.A.: First theoretical framework of triphenylamine–dicyanovinylene-based nonlinear optical dyes: structural modification of π-linkers. J. Phys. Chem. C **122**(7), 4009–4018 (2018)

Khan, M.U., Ibrahim, M., Khalid, M., Braga, A.A.C., Ahmed, S., Sultan, A.: Prediction of second-order nonlinear optical properties of D–π–A compounds containing novel fluorene derivatives: a promising route to giant hyperpolarizabilities. J. Cluster Sci. **30**(2), 415–430 (2019a)

Khan, M.U., Ibrahim, M., Khalid, M., Jamil, S., Al-Saadi, A.A., Janjua, M.R.S.A.: Quantum chemical designing of indolo [3, 2, 1-jk] carbazole-based dyes for highly efficient nonlinear optical properties. Chem. Phys. Lett. **719**, 59–66 (2019b)

Khan, M.U., Ibrahim, M., Khalid, M., Qureshi, M.S., Gulzar, T., Zia, K.M., Al-Saadi, A.A., Janjua, M.R.S.A.: First theoretical probe for efficient enhancement of nonlinear optical properties of quinacridone based compounds through various modifications. Chem. Phys. Lett. **715**, 222–230 (2019c)

Kovačević, N., Kokalj, A.: Analysis of molecular electronic structure of imidazole-and benzimidazole-based inhibitors: a simple recipe for qualitative estimation of chemical hardness. Corros. Sci. **53**(3), 909–921 (2011)

Lesar, A., Milošev, I.: Density functional study of the corrosion inhibition properties of 1, 2, 4-triazole and its amino derivatives. Chem. Phys. Lett. **483**(4–6), 198–203 (2009)

Lin, F., Jiang, K., Kaminsky, W., Zhu, Z., Jen, A.K.-Y.: A non-fullerene acceptor with enhanced intermolecular π-core interaction for high-performance organic solar cells. J. Am. Chem. Soc. **142**(36), 15246–15251 (2020)

Liu, Q., Wang, Q., Xu, M., Liu, J., Liang, J.: DFT characterization and design of anthracene-based molecules for improving spectra and charge transfer. Spectrochim. Acta Part A Mol. Biomol. Spectrosc. **227**, 117627–117627 (2020)

Muhammad, S., Janjua, M.R.S.A., Su, Z.: Investigation of dibenzoboroles having π-electrons: toward a new type of two-dimensional NLO molecular switch? J. Phys. Chem. C **113**(28), 12551–12557 (2009)

Muhammad, S., Xu, H.-L., Zhong, R.-L., Su, Z.-M., Al-Sehemi, A.G., Irfan, A.: Quantum chemical design of nonlinear optical materials by sp 2-hybridized carbon nanomaterials: issues and opportunities. J. Mater. Chem. C **1**(35), 5439–5449 (2013)

Nagarajan, B., Kushwaha, S., Elumalai, R., Mandal, S., Ramanujam, K., Raghavachari, D.: Novel ethynyl-pyrene substituted phenothiazine based metal free organic dyes in DSSC with 12% conversion efficiency. J. Mater. Chem. A **5**(21), 10289–10300 (2017)

Namuangruk, S., Fukuda, R., Ehara, M., Meeprasert, J., Khanasa, T., Morada, S., Kaewin, T., Jungsuttiwong, S., Sudyoadsuk, T., Promarak, V.: D-D− π–A-Type organic dyes for dye-sensitized solar cells with a potential for direct electron injection and a high extinction coefficient: synthesis, characterization, and theoretical investigation. J. Phys. Chem. C **116**(49), 25653–25663 (2012)

Panneerselvam, M., Kathiravan, A., Solomon, R.V., Jaccob, M.: The role of π-linkers in tuning the optoelectronic properties of triphenylamine derivatives for solar cell applications–A DFT/TDDFT study. Phys. Chem. Chem. Phys. **19**(8), 6153–6163 (2017)

Papadopoulos, M.G., Sadlej, A.J., Leszczynski, J.: Non-Linear Optical Properties of Matter. Springer (2006)

Parr, R.G., Donnelly, R.A., Levy, M., Palke, W.E.: Electronegativity: the density functional viewpoint. J. Chem. Phys. **68**(8), 3801–3807 (1978)

Parr, R.G., Szentpály, L.V., Liu, S.: Electrophilicity index. J. Am. Chem. Soc. **121**(9), 1922–1924 (1999)
Peng, Z., Yu, L.: Second-order nonlinear optical polyimide with high-temperature stability. Macromolecules **27**(9), 2638–2640 (1994)
Prasad, P.N., Williams, D.J.: Introduction to Nonlinear Optical Effects in Molecules and Polymers, vol. 1. Wiley, New York (1991)
Qin, C., Clark, A.E.: DFT characterization of the optical and redox properties of natural pigments relevant to dye-sensitized solar cells. Chem. Phys. Lett. **438**(1–3), 26–30 (2007)
Reed, A.E., Curtiss, L.A., Weinhold, F.: Intermolecular interactions from a natural bond orbital, donor-acceptor viewpoint. Chem. Rev. **88**(6), 899–926 (1988)
Reis, H., Papadopoulos, M.G., Munn, R.: Calculation of macroscopic first-, second-, and third-order optical susceptibilities for the urea crystal. J. Chem. Phys. **109**(16), 6828–6838 (1998)
Roy, R.S., Nandi, P.K.: Exploring bridging effect on first hyperpolarizability. RSC Adv. **5**(125), 103729–103738 (2015)
Shahid, M., Salim, M., Khalid, M., Tahir, M.N., Khan, M.U., Braga, A.A.C.: Synthetic, XRD, non-covalent interactions and solvent dependent nonlinear optical studies of Sulfadiazine-Ortho-Vanillin Schiff base:(E)-4-((2-hydroxy-3-methoxy-benzylidene) amino)-N-(pyrimidin-2-yl) benzene-sulfonamide. J. Mol. Struct. **1161**, 66–75 (2018)
Szafran, M., Komasa, A., Bartoszak-Adamska, E.: Crystal and molecular structure of 4-carboxypiperidinium chloride (4-piperidinecarboxylic acid hydrochloride). J. Mol. Struct. **827**(1–3), 101–107 (2007)
Tamer, Ö., Avcı, D., Atalay, Y.: Synthesis, X-Ray crystal structure, photophysical characterization and nonlinear optical properties of the unique manganese complex with picolinate and 1, 10 phenantroline: toward the designing of new high NLO response crystal. J. Phys. Chem. Solids **99**, 124–133 (2016)
Tsutsumi, N., Morishima, M., Sakai, W.: Nonlinear optical (NLO) polymers. 3. NLO polyimide with dipole moments aligned transverse to the imide linkage. Macromolecules **31**(22), 7764–7769 (1998)
Valverde, C., e Castro, S.A., Vaz, G.R., de Almeida Ferreira, J.L., Baseia, B., Osório, F.A.: Third-order nonlinear optical properties of a carboxylic acid derivative. Acta Chim. Slov. **65**(3), 739–749 (2018)
Wadsworth, A., Moser, M., Marks, A., Little, M.S., Gasparini, N., Brabec, C.J., Baran, D., McCulloch, I.: Critical review of the molecular design progress in non-fullerene electron acceptors towards commercially viable organic solar cells. Chem. Soc. Rev. **48**(6), 1596–1625 (2019)
Weinhold, F., Landis, C.R.: Valency and Bonding: A Natural Bond Orbital Donor-Acceptor Perspective. Cambridge University Press (2005)
Wielopolski, M., Kim, J.H., Jung, Y.S., Yu, Y.J., Kay, K.Y., Holcombe, T.W., Zakeeruddin, S.M., Grätzel, M., Moser, J.E.: Position-dependent extension of π-conjugation in D–π–A dye sensitizers and the impact on the charge-transfer properties. J. Phys. Chem. C **117**(27), 13805–13815 (2013)
Yamashita, S.: A tutorial on nonlinear photonic applications of carbon nanotube and graphene. J. Lightwave Technol. **30**(4), 427–447 (2011)
Zhang, B., Shi, G., Yang, Z., Zhang, F., Pan, S.: Fluorooxoborates: beryllium-free deep-ultraviolet nonlinear optical materials without layered growth. Angew. Chem. Int. Ed. **56**(14), 3916–3919 (2017)
Zhurko, G., Zhurko, D.: ChemCraft, version 1.6 (2009). URL: http://www.chemcraftprog.com

Authors and Affiliations

Muhammad Khalid[1,2] · Samran Naseer[1,2] · Muhammad Suleman Tahir[3] · Iqra shafiq[1,2] · Khurram Shahzad Munawar[4] · Sara Figueirêdo de Alcântara Morais[5] · Ataualpa A. C. Braga[5]

[1] Institute of Chemistry, Khwaja Fareed University of Engineering & Information Technology, Rahim Yar Khan 64200, Pakistan

[2] Centre for Theoretical and Computational Research, Khwaja Fareed University of Engineering &

Information Technology, Rahim Yar Khan 64200, Pakistan

[3] Institute of Chemical and Environmental Engineering, Khwaja Fareed University of Engineering & Information Technology, Rahim Yar Khan 64200, Pakistan

[4] Department of Chemistry, University of Sargodha, Sargodha, Pakistan

[5] Departamento de Química Fundamental, Instituto de Química, Universidade de São Paulo, Av. Prof. Lineu Prestes, 748, São Paulo 05508-000, Brazil